Impact Behavior of High Velocity Bird on a Flat Barrier

Sd. Abdul Kalam[1] ,
Assistant Professor
PVP Siddhartha Institute of Technology, Kanuru, Vijayawada, India

R Vijaya Kumar[2],
Manager
Rotary Wing R&D Center
Hindustan Aeronautics Limited, Bangalore, India

G Ranga Janardhana[3]
Professor & Director of IST
Jawaharlal Nehru Technological University Kakinada, Kakinada, India

Abstract:

In transient dynamic analysis of soft body impact, the contact and target surfaces impact each other with nonzero relative velocities and momentum, energy balance and thermodynamic equilibrium need to be satisfied. This helps to more accurately predict the duration of impact. The aircraft structure absorbs impact energy due to ingested birds, ice balls or hail stone and hard body objects, etc. This paper deals with a sensitivity study of hydrodynamic bird models which is performed by numerical simulation. The analysis is carried out by using an explicit Finite Element Analysis (FEA) code AUTODYNE for impact of substitute birds on square plate of rigid aluminium. The bird body is modeled as a porous water-air material in the shape of a flat or hemi-spherically ended cylinder. The finite element bird modeling was carried out by the use of the Smooth Particle Hydrodynamics (SPH) method for materials of different porosity. The energy and momentum variations with time are achieved from different porosities of two bird models are presented.

Keywords: ***Impact, Birds, Modelling, FEA, Hydrodynamic theory***

1. Introduction:

Ever since man put airplanes into the air, they have had the most unfortunate tendency to prematurely come down for various reasons, some of them more life threatening than others. The fact that airspace has to be shared with birds is not alien to that.

Bird impact usually occurs during taking off or landing of flights. Bird-strike is a serious and damaging event that must be accounted for in the design of flight critical aircraft components. The problem goes back to the dawn of modern aviation, when the Wright Brothers recorded the first bird -strike on 7 September 1905[1]. Although definitive figures are hard to obtain due to variations in reporting requirements, it is estimated that bird-strike events occur at least once in every two thousand flights. In civil aviation, more than 50 planes and over 223 lives are reported to have been lost since 1912 due to bird-strike. The cost to the worldwide aviation industry is estimated to be over USD 1 billion per-year [2].The collisions between birds and aircraft are known to cause substantial losses to the aviation industry in terms of damage and delays every year.

The ability of critical structure to withstand bird-strike events is regulated under the certification requirements. An accurate simulation of the bird strike is still a challenge when

applying numerical methods due to the complex physical phenomena which need to be correctly simulated in order to predict the response of the impacted structure. Nonlinear explicit finite element analyses enable prediction of damage caused by the foreign object impact without the need for costly and time consuming experiments. This ability is particularly useful in the certification phase of the design process, in which the compliance with certification requirements has to be demonstrated. Numerical methods and techniques are therefore still being improved in order to enhance the accuracy of bird impact simulations and, consequently, reduce the requirements for gas-gun experiments.

During the certification process, an aircraft must demonstrate its ability to land safely after being struck by a bird anywhere on the structure, at normal operating speeds [3]. Although substantial and costly damage may occur, the performance of the key components, including the wing, cowling and engines, must be demonstrated. Impacted components must maintain structural integrity during the large transient loading resulting from bird strike loads. Past experience has been to demonstrate this compliance through full-scale tests. Because of the costs and time involved, there is a need to improve modelling capabilities and enable verification by numerical methods. This in turn will help to decrease the number of destructive testing required. To accurately predict the response of an aircraft structure under impact loading, it is essential to have an accurate bird model.

Bird strike modelling has evolved remarkably since its first attempts, where a pressure pulse was applied to a finite element model [4]. Nowadays, the bird strike event represents a complex problem that the Lagrangian [5]-[12], the arbitrary Lagrangian-Euler [7]-[9], [13]-[15], and the smooth particle hydrodynamic bird model [4], [16]-[21] have successively attempted to solve with their own measure of success.

This paper aims at summarizing the steps involved in creating the bird model. It describes the theory of the bird strike and provides a sample of the available experimental data. Then a demonstration is given for a bird model based on: Variation of kinetic and internal energy and momentums with time for bird model.

Among the three modeling methods of bird mentioned earlier, SPH method is chosen with a brief parametric study of the factors influencing the fluid-structure interaction. They are compared and evaluated with respect to the theoretical information.

The rest of the paper is organized as follow: The next section covers the theory related to bird strike. The results obtained with the available models are presented. The conclusions are drawn in the last section.

2. Theory of Bird Strike

A bird undergoing impact at high velocity behaves as a highly deformable projectile where the yield stress is much lower than the sustained stress. Accordingly, the impact can be qualified as a hydrodynamic impact. That, and the fact that the density of flesh is generally close to the density of water, makes it possible for a bird to be considered as a lump of water hitting a target. This is the main assumption leading to the understanding of the behaviour of a bird.

P-alpha EOS

In the p-α model the compaction function defines the distension in terms of pressure, which conveniently expresses exactly what is measured in laboratory crush experiments. However, due to

the interdependence of pressure and distension, implementation of the p-α model in a hydrocode often requires iterative subcycling to find both simultaneously [22].

EOS of water and air

Additional useful information resulting from associating the bird to the water is the equation of state (EOS) used to describe the pressure-density (p-ρ) relationship in the bird medium. A few equations are available and the one most commonly used for the water-bird is a polynomial of degree 3 [23, 24]. This polynomial EOS for the bird model corresponds to a hydrodynamic, isotropic, and non-viscous constitutive law and is given as follows:

$$p = C_0 + C_1\mu + C_2\mu^2 + C3\mu^3 \ldots\ldots\ldots\ldots\ldots\ldots\ldots\ldots(1)$$

Where μ is given by $\mu=\rho/\rho_0-1$ and represents the change in density during the impact. This polynomial equation of state for the bird model corresponds to a hydrodynamic, isotropic, and non-viscous constitutive law.

The coefficients are given by expressions based on the initial density ρ_o, the speed of sound in water and an experimental constant k. The expressions are:

C_0-Initial Equilibrium Pressure, Considered to be

Negligible

$$C_1 = \rho_0 c_0^2, \qquad C_2 = (2k-1)C_1, \qquad C_3 = (k-1)(3k-1)C_1 \ldots\ldots\ldots\ldots\ldots\ldots(2)$$

where is: ρ_0 - density of the medium (for the water $\rho_{0,w}$ = 1000 kg/m^3 and for the air $\rho_{0,a}$ = 1.225 kg/m^3), c_0 - speed of the sound in the medium (for the water $c_{0,w}$ = 1483 m/s and for the air $c_{0,a}$ = 342 m/s) and k - experimental constant (for the water k_w = 2.0 and for the air k_a = 1.03).

EOS of porous material

The EOS of porous material is based on the thermodynamic equation that describes the state of matter under a given set of physical conditions. It is a constitutive equation that provides a mathematical relationship between two or more state functions such as the temperature T, the

Volume V or density, pressure and internal energy:

$$p = p\,(\rho, E) = p(V, E) = p(\rho, T) = (V, T) \ldots\ldots\ldots\ldots\ldots\ldots(3)$$

Further development of the theory for porous medium requires the elastic bulk modulus and the sound speed of porous to be defined. The sound speed is calculated assuming:

$$c_{por} = (1-z)^m c_{o,w} + z c_{o,a} \ldots\ldots\ldots\ldots\ldots\ldots(4)$$

The diagram in Fig.1 illustrates the developed distribution for the exponent values m =1-5, and m = 10.

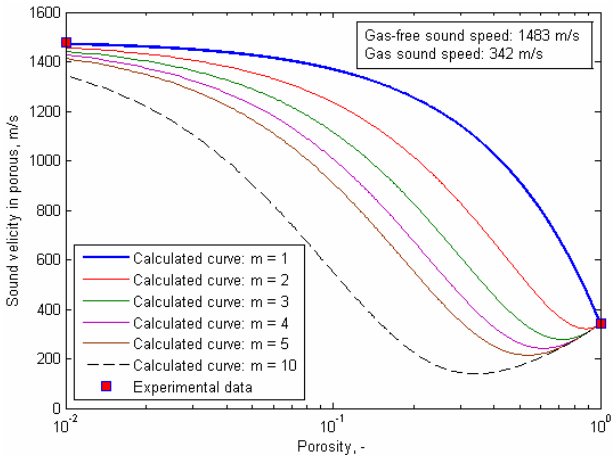

Fig. 1. Sound speed distribution depending on porosity

3. FEM modeling:

Bird model

For a *bird material* a homogeneous mixture of water and air was used. The porosity (volume presence of the air) varied from z = 0.0 to z = 0.4. The effect of porosity with the P-alpha EOS for porous material was investigated. The appropriate mechanical parameters of the water and the water-air mixture depending on porosity are given in Table 1.

Table 1. Mechanical parameters of the water and the water-air mixture

Porosity z	Density ρ	Sound speed c_p (for m=1)	Bulk modulus K (for m=1)
--	kg/m^3	m/s	MPa
0.0	1000.0	1483	2200
0.1	900.12	1368	1668
0.2	800.25	1256	1260
0.3	700.37	1142	907
0.4	600.49	1026	632

For the purpose of this research, two typical *bird shapes* generally used in the bird strike analysis, a flat and a hemispherical cylinder were considered. In each case, the height and the diameter of the bird was assumed to be 200 mm and 100 mm, respectively. The length-to-diameter ratio of 2 for each bird shape was identical.

Two types of the numerical models of body shapes based on the SPH particles distributions along the symmetry axis are presented in Fig.2.

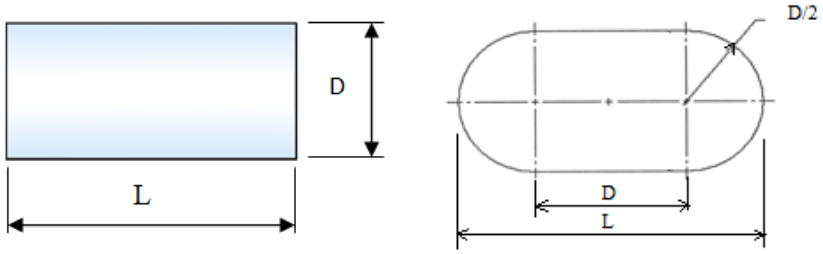

(a) Cylindrical **(b) Cylindrical with hemispherical ends**

Fig. 2. Substitute bird geometries *Target model*

For simplicity, the target structure was initially assumed to be rigid. Aluminium plate (AL 1100-O), with the dimensions 700x700x10 mm modeled as a rigid target body to decouple between the impact loads and the target deflection. All degrees of freedom of the target structure were constrained. The appropriate mechanical parameters of the AL 1100-O are given in Table 2.

Table 2. Mechanical parameters of the AL 1100-O target structure

Density ρ	Poisson's Ratio (μ)	Shear Modulus G	Tensile yield Strength (R_{eH})	Melting Temp. (T_{melt})
(Kg/m^3)		GPa	GPa	^0C
2707	0.3	27.1	0.48	946.85

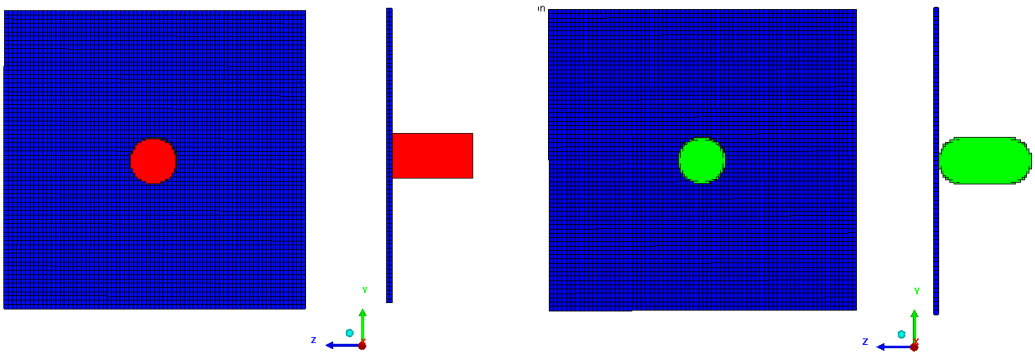

Fig. 3. Lagrangian model of a rigid target and an SPH model of a cylindrical and Cylindrical with hemispherical ends projectile

4. Results and discussion

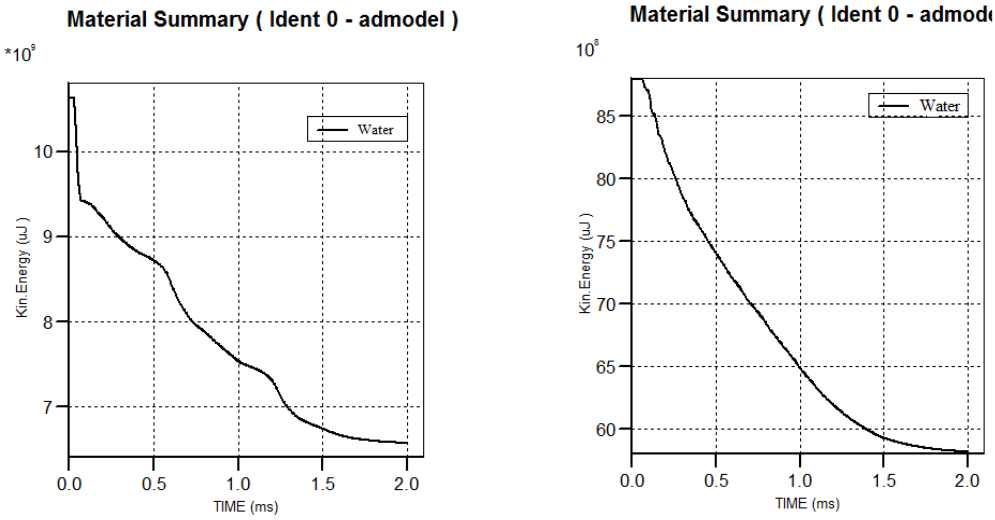

Fig. a) Cylindrical **Fig. b) Cylindrical with hemispherical ends**

Fig.4. Comparison of Kinetic Energy with time of cylindrical and Cylindrical with hemispherical ends projectiles with porosity z=0.0 and impact velocity V_{im}=116m/s.

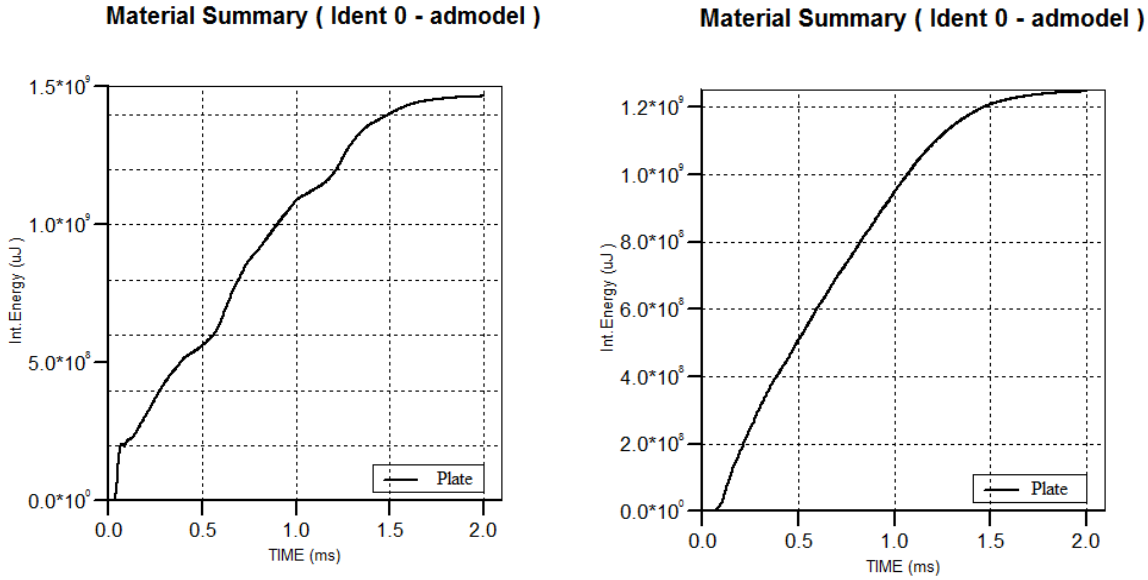

Fig. a) Cylindrical **Fig. b) Cylindrical with hemispherical ends**

Fig.5.Comparison of Internal Energy with time absorbed by target structure impacted by cylindrical and Cylindrical with hemispherical ends projectile with porosity z=0.0 and impact velocity V_{im}=116m/s.

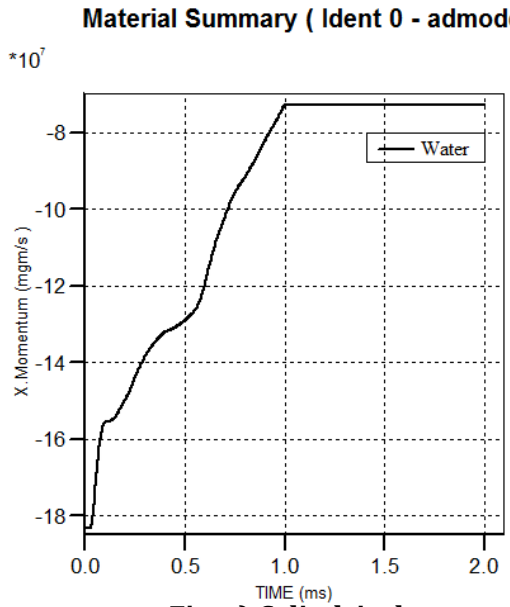

Fig. a) Cylindrical

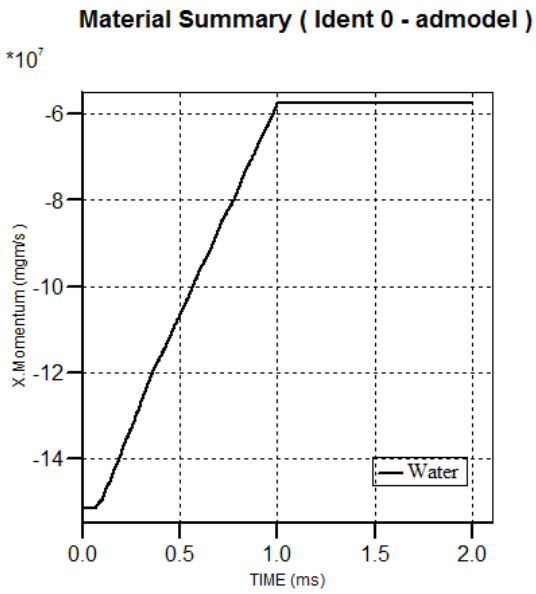

Fig. b) Cylindrical with hemispherical ends

Fig.6. Comparison of Momentums of a cylindrical and Cylindrical with hemispherical ends projectile with porosity z=0.0 and impact velocity V_{im}=116m/s

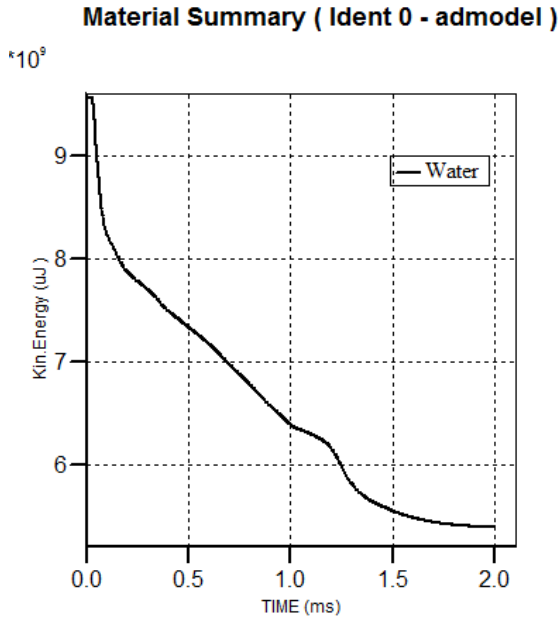

Fig. a) Cylindrical

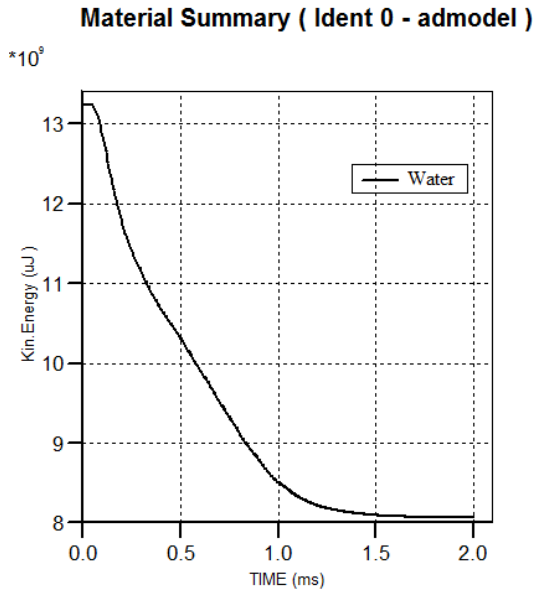

Fig. b) Cylindrical with hemispherical ends

Fig.7. Comparison of Kinetic Energy with time of cylindrical and Cylindrical with hemispherical ends projectile with porosity z=0.1 and impact velocity V_{im}=116m/s.

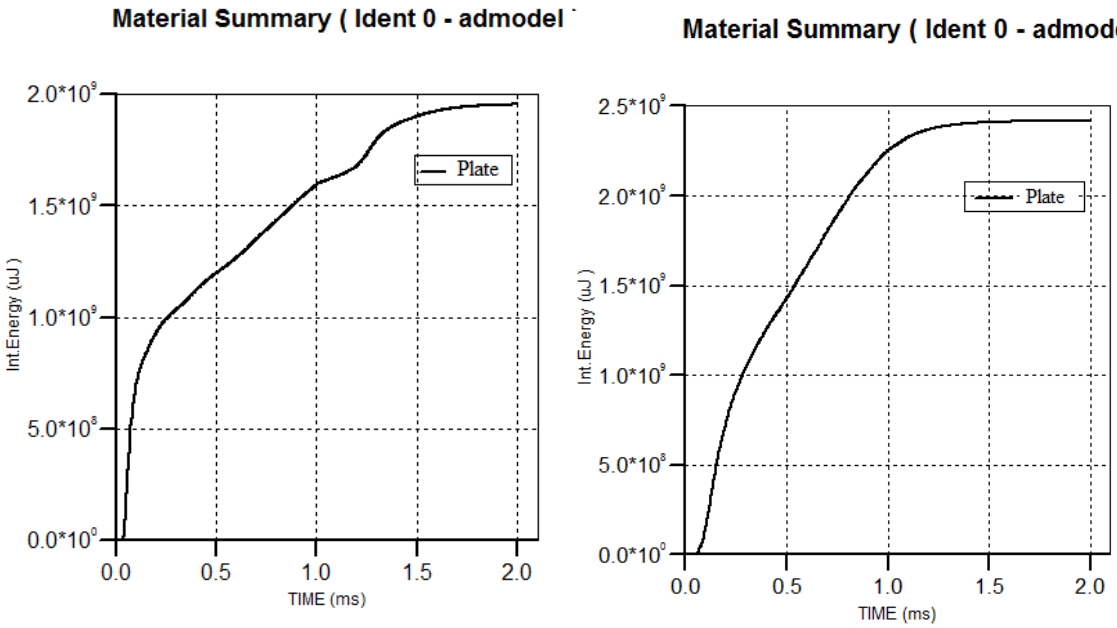

Fig. a) Cylindrical **Fig. b) Cylindrical with hemispherical ends**

Fig.8. Comparison of Internal Energy with time absorbed by target structure impacted by cylindrical and Cylindrical with hemispherical ends projectile with porosity z=0.1 and impact velocity V_{im}=116m/s

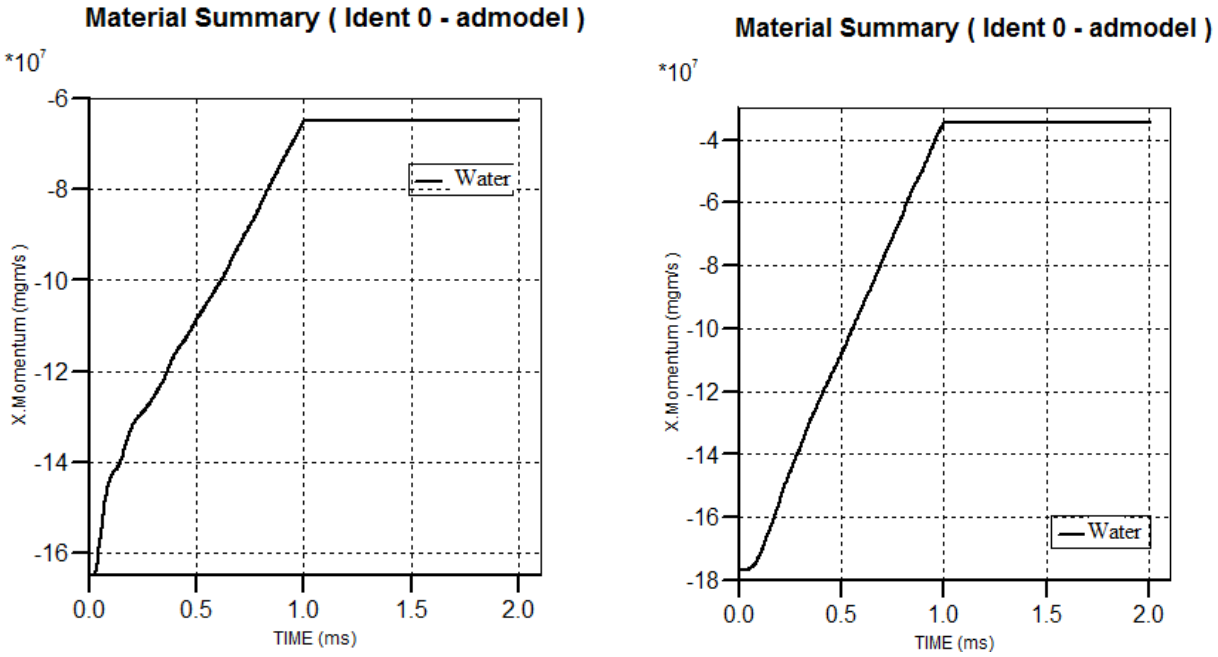

Fig. a) Cylindrical **Fig. b) Cylindrical with hemispherical ends**

Fig.9. Comparision of Momentums of a cylindrical and Cylindrical with hemispherical ends projectile with porosity z=0.1 and impact velocity V_{im}=116m/s.

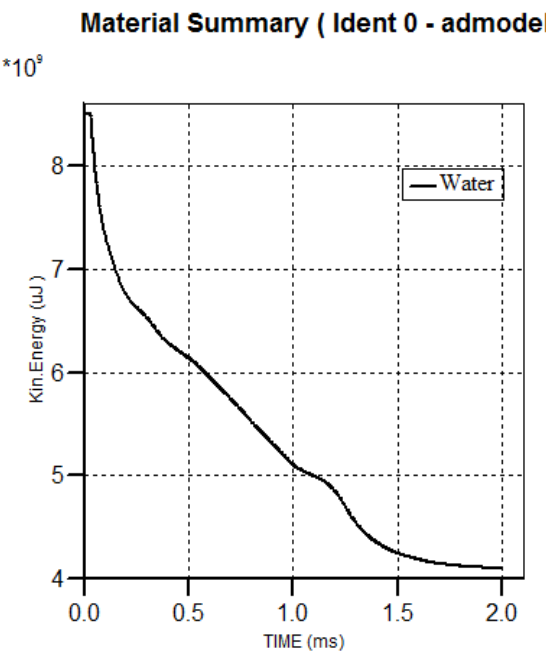

Fig. a) Cylindrical

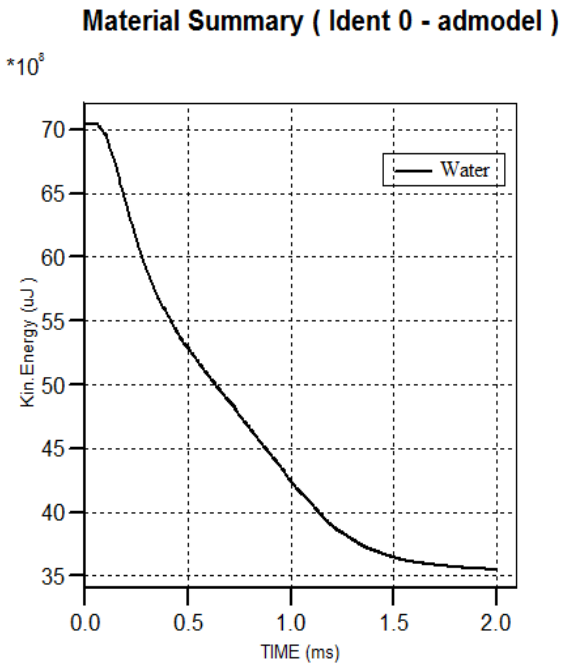

Fig. b) Cylindrical with hemispherical ends

Fig. 10. Comparison of Kinetic Energy with time of cylindrical and Cylindrical with hemispherical ends projectile with porosity z=0.2 and impact velocity V_{im}=116m/s.

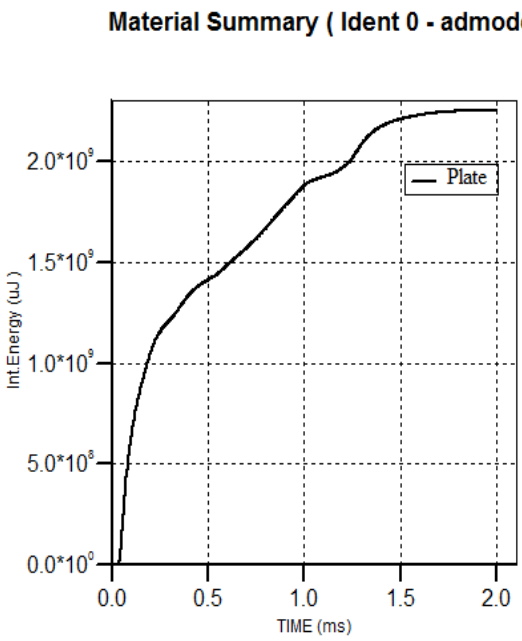

Fig. a) Cylindrical

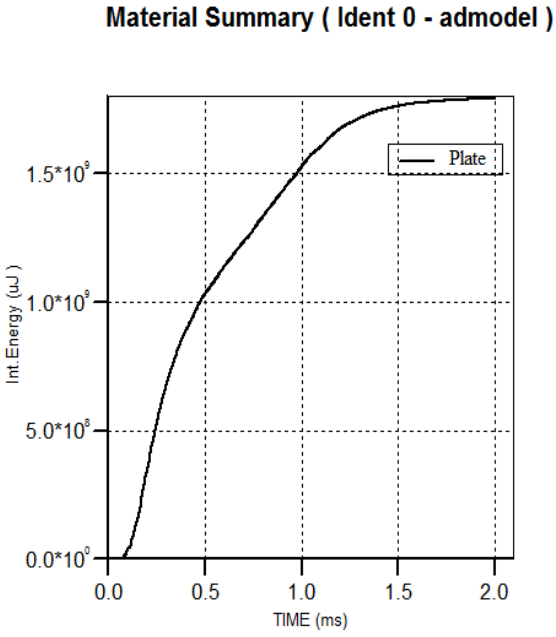

Fig. b) Cylindrical with hemispherical ends

Fig.11. Comparison of Internal Energy with time absorbed by target structure impacted by cylindrical and Cylindrical with hemispherical ends projectile with porosity z=0.2 and impact velocity V_{im}=116m/s.

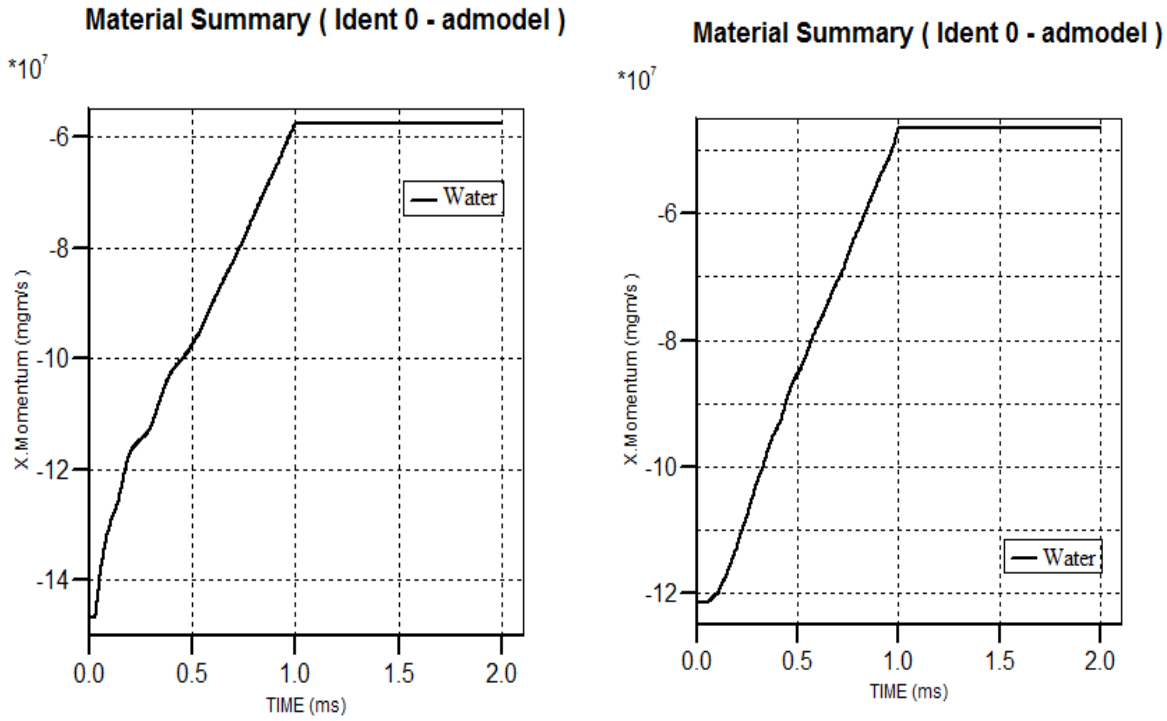

Fig. a) Cylindrical **Fig b) Cylindrical with hemispherical ends**

Fig. 12. Comparison of Momentums of a cylindrical and Cylindrical with hemispherical ends projectile with porosity z=0.2 and impact velocity V_{im}=116m/s.

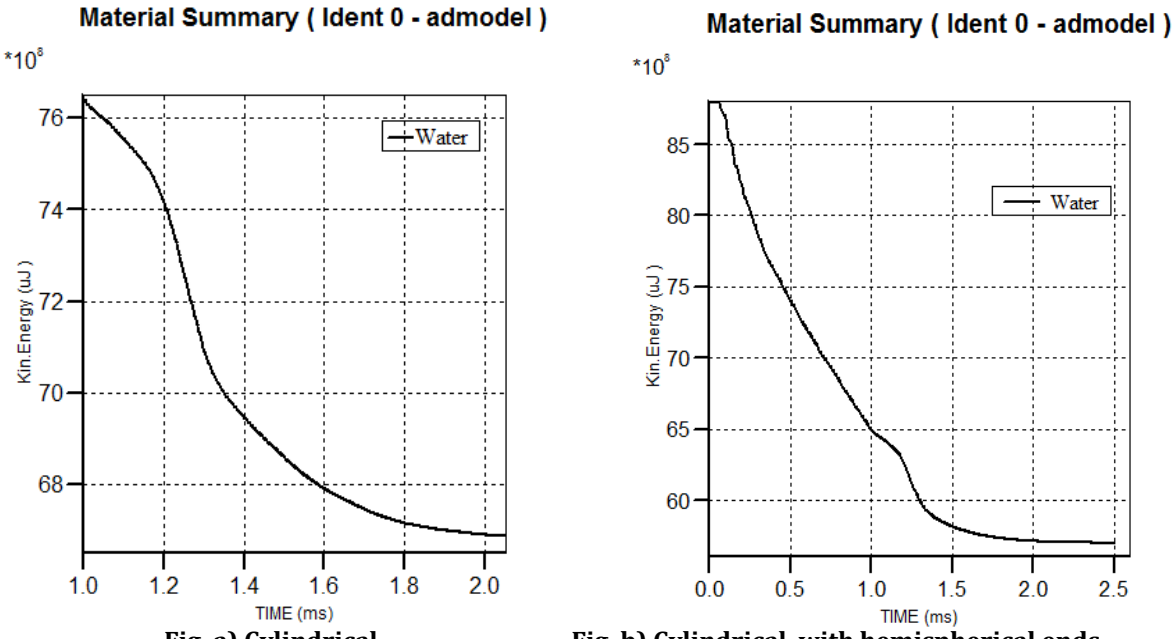

Fig. a) Cylindrical **Fig. b) Cylindrical with hemispherical ends**

Fig.13. Comparison of Kinetic Energy with time of cylindrical and Cylindrical with hemispherical ends projectile with porosity z=0.3 and impact velocity V_{im}=116m/s.

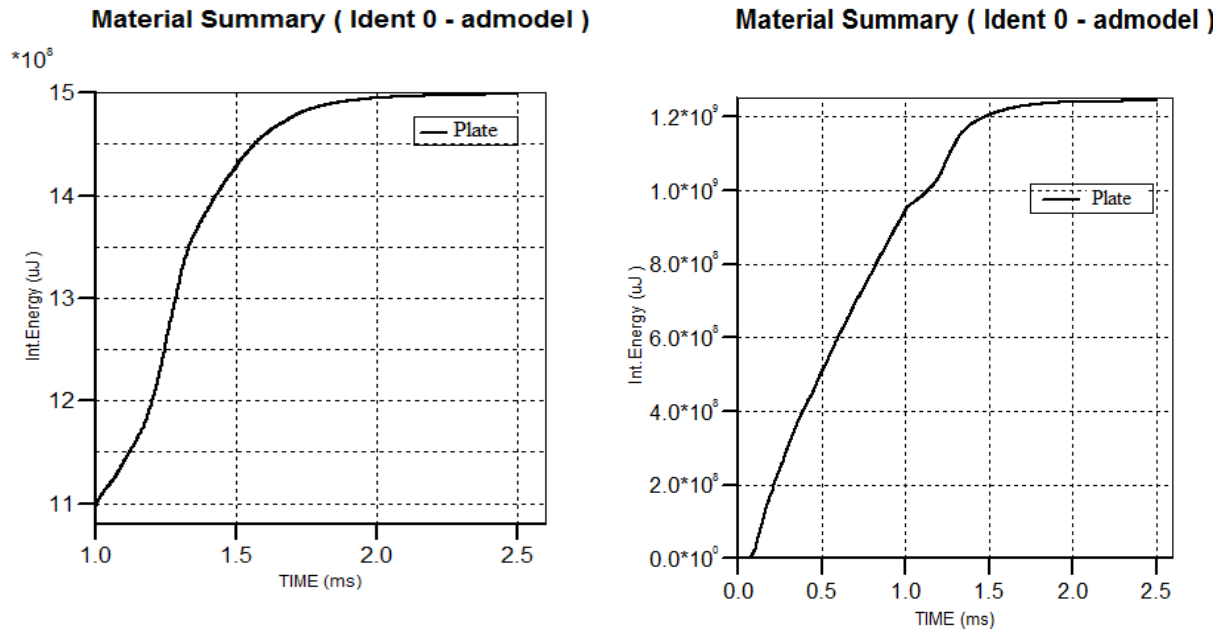

Fig. a) Cylindrical **Fig. b) Cylindrical with hemispherical ends**

Fig.14. Comparison of Internal Energy with time absorbed by target structure impacted by cylindrical and Cylindrical with hemispherical ends projectile with porosity z=0.3 and impact velocity V_{im}=116m/s.

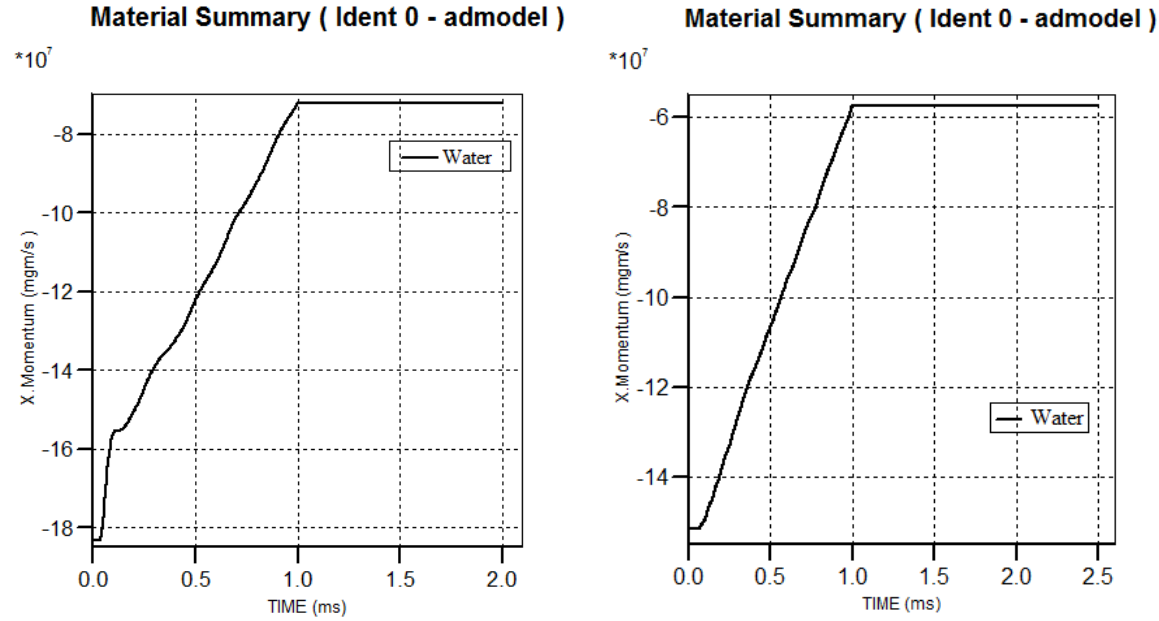

Fig. a) Cylindrical **Fig. b) Cylindrical with hemispherical ends**

Fig.15. Comparison of Momentums of a cylindrical and Cylindrical with hemispherical ends projectile with porosity z=0.3 and impact velocity V_{im}=116m/s

.

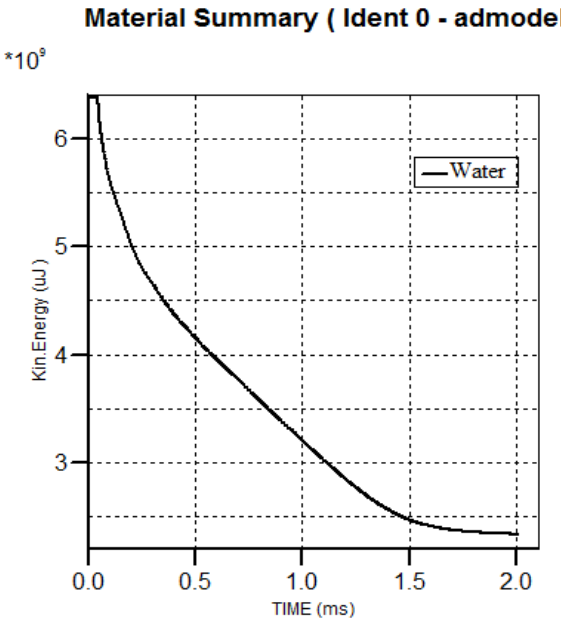

Fig. a) Cylindrical

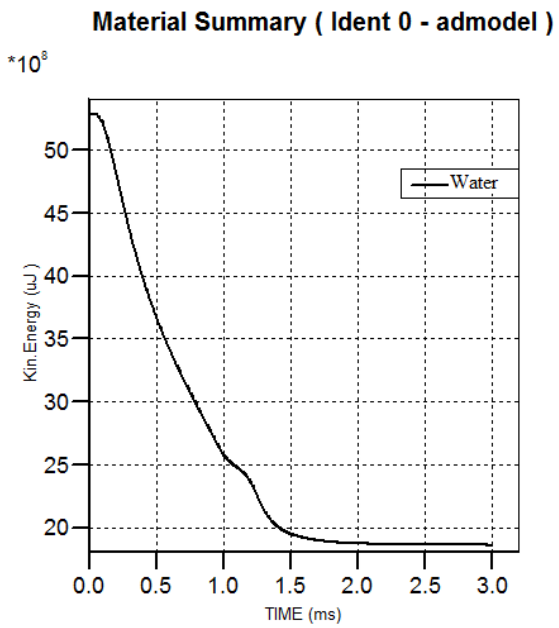

Fig. b) Cylindrical with hemispherical ends

Fig.16. Comparison of Kinetic Energy with time of cylindrical and Cylindrical with hemispherical ends projectile with porosity z=0.4 and impact velocity V_{im}=116m/s.

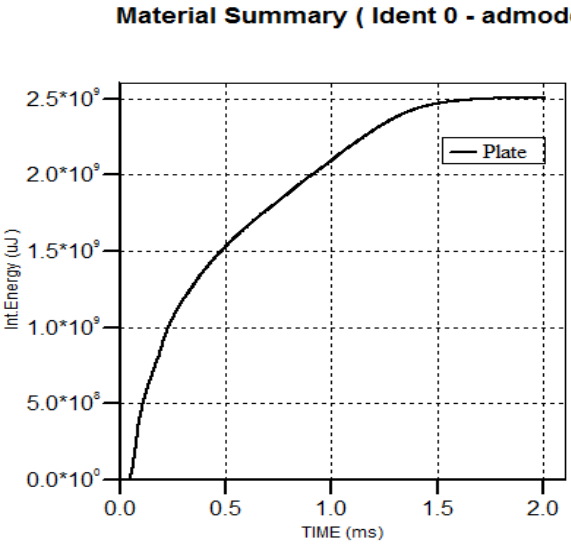

Fig. a) Cylindrical

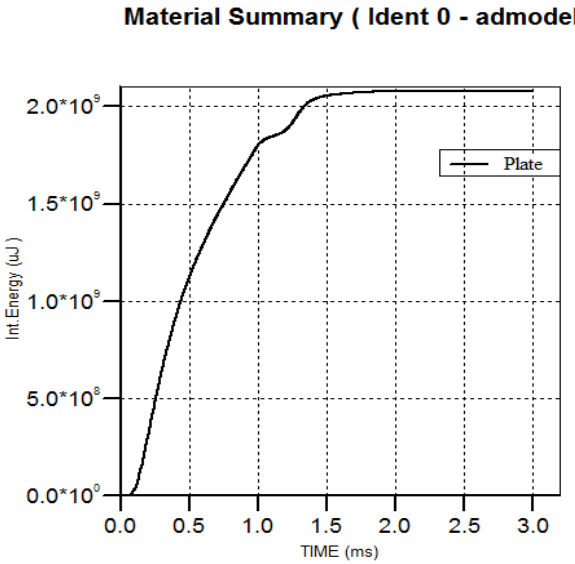

Fig. b) Cylindrical with hemispherical ends

Fig.17. Comparison of Internal Energy with time absorbed by target structure impacted by cylindrical and Cylindrical with hemispherical ends projectile with porosity z=0.4 and impact velocity V_{im}=116m/s.

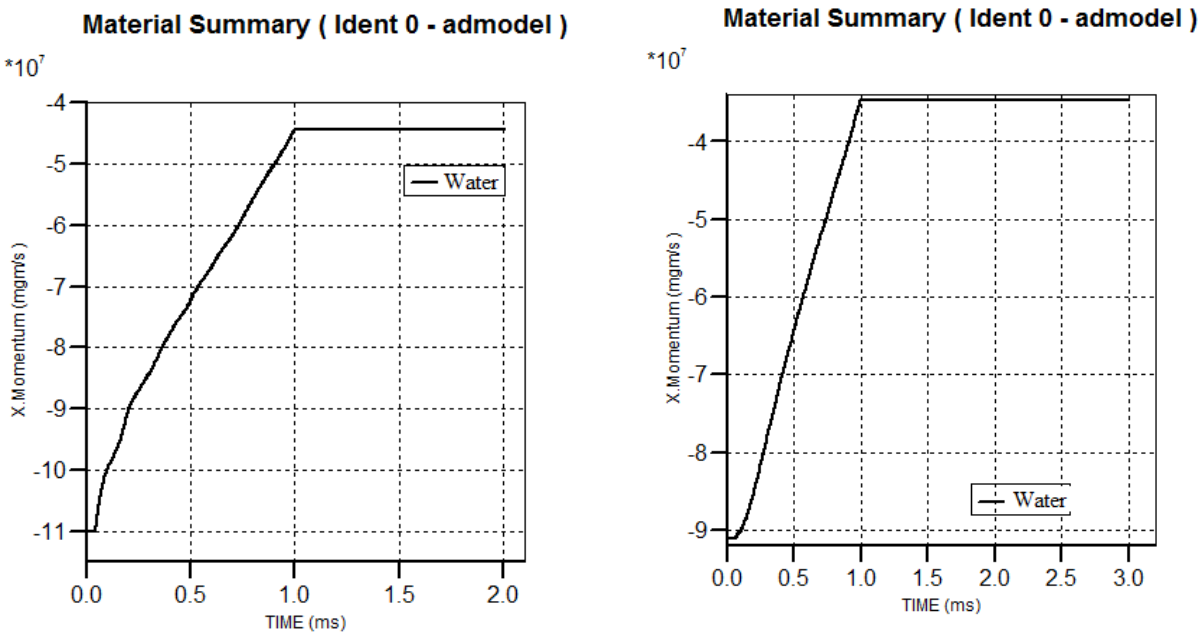

Fig. a) Cylindrical **Fig. b) Cylindrical with hemispherical ends**

Fig.18. Comparison of Momentums of a cylindrical and Cylindrical with hemispherical ends projectile with porosity z=0.4 and impact velocity V_{im}=116m/s.

Comparing the results of the numerical simulations of the bird impact on the rigid target, for a flat cylinder and a hemispherical cylinder shape of the bird body, gives the following:

-Maximum Kinetic Energy distributions (Figures 4, 7, 10, 13 and 16) comparing the flat cylinder impact shows 26.66% higher Kinetic Energy values than in the case of the hemispherical ended cylinder impact;

-Internal Energy absorbed by the metallic plate (Figures 5, 8, 11, 14 and 17) comparing the flat cylinder impact shows 13.79% higher values than in the case of the hemispherical ended cylinder impact; and

-Momentums of the projectile (Figures 6, 9, 12, 15 and 18) comparing the flat cylinder impact shows 17.24% higher values than in the case of the hemispherical ended cylinder impact.

5. Conclusions

A homogeneous water-air mixture was used for the bird material and the equation for the elastic bulk modulus and the sound speed of porous medium depending on porosity was involved in the analysis.

Finite element numerical simulations of the bird impact were carried out by the SPH method to represent the bird body. Based on the mechanical parameters, determined by the proposed equation, the effect of porosity with the P-alpha EOS for porous materials was tested.

The numerical simulation of various cases of the bird impact including the variation of bird material density, shape and impact velocity, and target plate parameters was successfully performed.

Regarding the shape, it can be seen that the predicted energies and momentums associated with two bird shapes, among these, the cylindrical with hemispherical ended bird shape with porosities 0.3 and 0.4 results gives very nearer to experimental values[24].

6. References

[1]Sharing the skies manual. TP13549. Transport Canada; 2004.
[2]Completeness and accuracy of birdstrike reporting in the UK. CAA Paper 2006/05. UK: Civil Aviation Authority; 2006.
[3]Federal Aviation Administration, *Policy for Bird Strike*, (U.S. Department of Transportation, 2002)
[4]M.A. McCarthy, J.R. Xiao, C.T. McCarthy, A. Kamoulakos, J. Ramos, J.P. Gallard, V. Melito, Modeling of Bird Strike on an Aircraft Wing Leading Edge Made from Fibre Metal Laminates – Part 2: Modeling of Impact with SPH Bird Model, *Applied Composite Materials*, Vol. 11, pp.317-340, 2004
[5]L.Iannucci, *Bird-strike impact modeling*, Seminar Foreign Object Impact and Energy Absorbing Structure, London, England, 1998, pp. 11-29
[6]E. Niering, Simulation of Bird Strikes on Turbine Engines, *Journal of engineering for gas Turbine and Power*, Vol. 11, pp. 572-5782, 1990
[7]B. Langrand, A.-S. Bayart, Y. Chaveau, E. Deletombe, Assessment of Multi-Physics FE Methods for Bird Strike Modeling – Application to a Metallic Riveted Airframe, *International Journal of Crashworthiness*, Vol. 7, pp. 415-428, 2002.
[8]Alan Dobyns, *Bird Strike Analysis of S-92 Vertical Tail Cover Using DYTRAN*, AHS Affordable Composite Structures Conference, Bridgeport, 1998.
[9]Alan Dobyns, Frank Frederici, Robert Young, *Bird Strike Analysis and Test of a Spinning S-92 Tail Rotor*, American Helicopter Society 57th Annual Forum, Washington, 2001.
[10]Airoldi, B. Cacchione, Modeling of Impact Forces and Pressures in Lagrangian Bird Strike Analyses, *International Journal of Impact Engineering*, Vol. 32, pp. 1651-1677, 2006.
[11]Erkan Kirtil, Dieter Pestal, Alexander Kollofrath, Nils Gänsicke, Josef Mendler, *Simulating the Impact Behaviour of Composite Aircraft Structures*, ABAQUS Users' Conference, Austria, 2003.
[12]Frederick Stoll, Robert A. Brockman, *Finite Element Simulation of High-Speed Soft-Body Impacts*, 38th AIAA/ ASME/ ASCE/ AHS/ ASC Structures, Structural Dynamics, and Material Conference, 1997, pp. 334-344
[13]A.G. Hanssen, Y. Girard, L. Olovsson, T. Berstad, M. Langseth, A numerical model for bird strike of aluminium foam-based sandwich panels, *International Journal of Impact Engineering*, Vol. 32, pp. 1127-1144, 2006.
[14]Stuart Kari, Jon Gabrys, David Lincks, *Birdstrike Analysis of Radome and Wing Leading Edge Using LS-DYNA*, 5th International LS-DYNA Users Conference, Southfield, 1998.
[15]S. C. McCallum, C. Constantinou, *The influence of bird-shape in bird-strike analysis*, 5th European LS-DYNA Users Conference, Birmingham ,2005
[16]TH. Kermanidis, G. Labeas, M. Sunaric, L. Ubels, Development and Validation of a Novel Bird Strike Resistant Composite Leading Edge Structure, *Applied Composite Materials*, Vol. 12, pp. 327-353, 2005.
[17]Alastair F. Johnson, Martin Holzapfel, Modeling Soft Body Impact on Composite Structures, *Composite Structures*, Vol. 61, pp. 103-113, 2003.
[18]N. F. Martin Jr., Nonlinear Finite-Element Analysis to Predict Fan-Blade Damage Due to Soft-Body Impact, *Journal of Propulsion*, Vol. 6, n. 4, pp. 445-450, 1990.
[19] D. Chevrolet, S. Audic, J. Bonini, *Bird Impact Analysis on a Bladed Disk*, Reduction of Military Vehicle Acquisition Time and Cost through Advanced Modeling and Virtual Simulation, Paris, 2002.
[20] M. A. McCarthy, R. J. Xiao, C. T. McCarthy, A. Kamoulakos, J. Ramos, J. P. Gallard, V. Melito, Modeling Bird Impacts on an Aircraft Wng- Part 2 Modeling the impact with and SPH bird model, *International Journal of Crashworthiness*, Vol. 10, n.1, pp. 51-59, 2005

[21] Th. Kermanidis, G. Labeas, M. Sunaric, A. F. Johnson, M. Holzapfel, Bird Strike Simulation on a Novel Composite Leading Edge Design, *International Journal of Crashworthiness*, Vol. 11, n. 3, pp. 189-201, 2006

[22]Kerley GI. 1992. Sandia National Lab Report, SAND 92-0553.

[23]IVANČEVIĆ,D., SMOJVER,I.: *Hybrid approach in bird strike damage prediction on aeronautical composite structures,* Composite Structures, 2011, 94, 1, pp.15-23.

[24]NIZAMPATMAN,L.S.: *Models and methods for bird strike load predictions*, PhD Dissertation, Faculty of Graduate School, Wichita State University, USA, (2007).

[25]Herrmann W. Constitutive Equation for the Dynamic Compaction of Ductile Porous Materials. *Journal of Applied Physics*, 1969; **40** (6), 2490-2499.

[26]Carroll MM, Holt AC. Static and Dynamic Pore-Collapse Relations for Ductile Porous Materials. *Journal of Applied Physics*, 1972; **43**(4), 1626-1636.